Burns & Trauma, 2020, 8, tkaa025
doi: 10.1093/burnst/tkaa025
Research Article

Research Article

CD26 upregulates proliferation and invasion in keloid fibroblasts through an IGF-1-induced PI3K/AKT/mTOR pathway

Yu Xin, Peiru Min, Heng Xu, Zheng Zhang*, Yan Zhang* and Yixin Zhang*

Department of Plastic and Reconstructive Surgery, Shanghai 9th People's Hospital, Shanghai Jiao Tong University School of Medicine, 639 Zhi Zao Ju Road, Shanghai, 200011, China

*Correspondence. Zheng Zhang, Email: zhangzheng958@163.com; Yan Zhang, Email: 13651817522@163.com; Yixin Zhang, Email: zhangyixin6688@163.com

Received 19 November 2019; Revised 7 April 2020; Editorial decision 2 June 2020

Abstract

Background: Keloid is a fibrotic dermal disease characterized by an abnormal increase in fibroblast proliferation and invasion. These pathological behaviours may be related to the heterogeneity of keloid fibroblasts (KFs); however, because of a lack of effective biomarkers for KFs it is difficult to study the underlying mechanism. Our previous studies revealed that the expansion of $CD26^+$ KFs was responsible for increased keloid proliferation and invasion capabilities; the intrinsic relationship and mechanism between CD26 and keloid is therefore worthy of further investigation. The aim of this study was to explore molecular mechanisms in the process of CD26 upregulated KFs proliferation and invasion abilities, and provide more evidence for CD26 as an effective biomarker of keloid and a new clinical therapeutic target.

Methods: Flow cytometry was performed to isolate $CD26^+/CD26^-$ fibroblasts from KFs and normal fibroblasts. To generate stably silenced KFs for CD26 and insulin-like growth factor-1 receptor (IGF-1R), lentiviral particles encoding shRNA targeting CD26 and IGF-1R were used for transfection. Cell proliferations were analysed by cell counting kit-8 assay and 5-ethynyl-2′-deoxyuridine (EdU) incorporation assay. Scratching assay and transwell assay were used to assess cell migration and invasion abilities. To further quantify the regulatory role of CD26 expression in the relevant signalling pathway, RT-qPCR, western blot, ELISA, PI3K activity assay and immunofluorescence were used.

Results: Aberrant expression of CD26 in KFs was proven to be associated with increased proliferation and invasion of KFs. Furthermore, the role of the IGF-1/IGF-1 receptor axis was also studied in CD26 and was found to upregulate KF proliferation and invasion. The PI3K/protein kinase B (AKT)/mammalian target of rapamycin (mTOR) pathway was shown to affect CD26-regulated KF proliferation and invasion by increasing phosphorylation levels of S6 kinase and 4E-binding protein.

Conclusions: CD26 can be the effective biomarker for KFs, and its expression is closely related to proliferation and invasion in keloids through the IGF-1-induced PI3K/AKT/mTOR pathway. This work provides a novel perspective on the pathological mechanisms affecting KFs and therapeutic strategies against keloids.

Key words: CD26, IGF-1, Invasion, Keloids, PI3K/AKT/mTOR signalling pathway, Proliferation, Fibroblast

© The Author(s) 2020. Published by Oxford University Press.
This is an Open Access article distributed under the terms of the Creative Commons Attribution Non-Commercial License (http://creativecommons.org/licenses/by-nc/4.0/), which permits non-commercial re-use, distribution, and reproduction in any medium, provided the original work is properly cited. For commercial re-use, please contact journals.permissions@oup.com

Downloaded from academic.oup.com/burnstrauma/article/doi/10.1093/burnst/tkaa025/5943291 by guest on 15 October 2026

Background

Keloids are benign fibro-proliferative tumours of the dermis. In histological terms, their central histopathologic hallmark is persistent activation, which releases excess extracellular matrix (ECM) components [1–3]. In pathological terms, they exhibit tumour-like progressive invasion of adjacent normal dermis [2, 4, 5]. Moreover, the enlarging and invasive capacity of keloids may also become symptomatic by causing deformity or limiting joint mobility. At present, there are many available therapeutic strategies to reduce the appearance and discomfort of keloids, among which surgical incision remains the most common method; however, surgical excision alone often leads to high recurrence. Other treatments include invasive approaches, such as topical drug injection, and non-invasive approaches, such as laser therapy, silicone treatment, cryotherapy and radiation therapy [6, 7]. Although multiple therapeutic methods are available the clinical results remain unsatisfactory [3]. Simultaneously, the adverse effects and complexity of current treatment methods result in poor patient compliance, thus the optimal treatment of keloids remains contentious.

More research focuses on the underlying pathogenic mechanisms for preventing and treating this disease [8]. It has been shown that the pathogenesis of keloids are related to fibroblast dysfunction [3]. Keloid fibroblasts (KFs), the special fibroblasts in keloid conditions, are considered to play a critical role in the formation of keloids. Although KFs have similar morphological characteristics to normal fibroblasts (NFs), they display specificity in aberrant proliferation and mediate the elevation of ECM and various cytokines during the formation of keloids. Furthermore, various cytokines, including transforming growth factor-β1 (TGF-β1), vascular endothelial growth factor (VEGF), platelet-derived growth factor (PDGF), interleukin-1(IL-1), inerleukin-6 (IL-6), tumor necrosis factor-α (TNF-α) and insulin-like growth factor-1 (IGF-1), have been considered to promote the formation of keloids [4, 9, 10]. Therefore, the pathological function of KFs can provide a novel method to treat keloids and is worthy of further study [11].

In recent years, cell heterogeneity has been considered to be closely related to scar formation [12, 13]; however, because of the lack of a specific marker it is difficult to identify subsets in keloid tissue, which is a significant barrier in keloid research [14].

At this point, CD26 may be a candidate due to its relationship with fibroblasts. CD26 is a type II transmembrane protein which can hydrolyse proline or alanine from the N-terminus of polypeptides [15]. CD26 can modulate T cell signal transduction processes as a co-stimulatory molecule [16] and enhance its expression in many autoimmune diseases [17, 18]. Treatment with DPP4 inhibitors could attenuate the tissue fibrosis in patients with diabetes mellitus [19]. Of particular interest, Rinkevich *et al.* successfully used CD26 to isolate a single fibroblast lineage with unique functions in skin fibrosis during embryonic development and pathological fibrogenesis, demonstrating that CD26 could be an effective functional marker for fibroblasts [12]; however, the role of CD26-expressing fibroblasts as a subset in keloids has not yet been validated. Thus, we analysed differences in expression of CD26 in KFs and NFs; results demonstrated that CD26 expression was upregulated in KFs compared to NFs [20]. Furthermore, the $CD26^+$ fibroblast subpopulation was proven to be more active in proliferation compared with the $CD26^-$ fibroblast population [20]; however, the underlying mechanism between CD26 and proliferation of KFs remains unknown. Furthermore, besides proliferation, keloids also display the prominent feature of invasion of surrounding normal skin, and the role of CD26 therein is also unknown. Therefore, it is necessary to study the underlying mechanism of CD26 in regulating the proliferation and invasion, which is of significance for the clinical treatment of keloids.

In many CD26-related fibrotic diseases, TGF-β signalling has emerged as a core pathway of fibroblast activation [13, 21, 22]. We speculate that there is another signalling pathway playing a key role in CD26 regulation in keloids, that of IGF-1 meditated. IGF-1 is mediated by the IGF-1 receptor (IGF-1R) and plays a key role in the initiation and termination of wound repair [23]. Compared to NFs, KFs have been proven to upregulate IGF-1 expression [24]. KFs overexpressing IGF-1R are resistant to apoptosis, resulting in persistent cell proliferation and excessive ECM deposition [25]. Moreover, IGF-1 binds to the IGF-1R and can activate the phosphatidylinositol 3-kinase (PI3K)/protein kinase B (AKT)/mammalian target of rapamycin (mTOR) pathway [26], which is involved in mediation of the invasiveness of KFs [27]. The PI3K/AKT/mTOR pathway exerts effects on parts of the wound healing process, such as cell migration, proliferation and ECM maturation [28], as well as keloid development [29].

In the present study, we first verified that CD26 expression in KFs was related to increased proliferation and invasion of KFs. Then the IGF-1/IGF-1R axis was proven to play a key role in the CD26-regulated KF proliferation and invasion processes. Then, the PI3K/AKT/mTOR pathway was verified to be involved in CD26-regulated KF proliferation and invasion-related signalling pathways. Our results indicate that CD26 expression is closely related to the aberrant proliferation and invasion of KFs and that targeting CD26 and other relevant signalling pathways may have a potential therapeutic effect on keloids.

Methods

Inhibitors and antagonist

LY294002, KU-0063794, AZD3463, SB505124, axitinib, tocilizumab and Bay 11-7085 were purchased from Selleck Chemicals (USA). Crenolanib (CP-868596) was purchased from MedChemExpress. AS101 was purchased from Cayman Chemical (USA). Stock solutions of compounds were prepared in DMSO and stored at −20°C or diluted in media for experiments.

Downloaded from academic.oup.com/burnstrauma/article/doi/10.1093/burnst/tkaa025/5943291 by guest on 15 October 2026

Table 1. Demographic data of keloid samples used in this study

Sample no.	Gender	Age	Site	Size of the specimens (cm)
K1	F	32	Abdomen	3×5
K2	F	25	Abdomen	2.5×3.5
K3	F	30	Abdomen	5×3.5
K4	M	35	Abdomen	10×3
K5	F	38	Abdomen	4×3
K6	M	42	Abdomen	4.5×2; 3×1
N1	F	45	Abdomen	6×3
N2	F	40	Abdomen	7×2
N3	F	28	Abdomen	6×3
N4	M	35	Abdomen	4×3
N5	F	38	Abdomen	5×3
N6	F	36	Abdomen	5×4

Samples K1-K6 and N1-N6 were used for flow cytometry analysis. Samples K1-K3 were used for cell counting kit-8 cell proliferation assay, EdU incorporation assay, cell migration assay and cell invasion assay. Samples K1, K2, K4 were used for RT-qPCR and western blot analysis. Samples K1, K3, K5 were used for ELISA assay and phosphatidylinositol 3-kinase activity assay. Samples K2, K5, K6 were used for immunocytofluorescence staining. Samples N2 and K1 were used for immunohistofluorescence staining

Tissue samples and cell culture

Keloid scar specimens were obtained from 6 patients (2 men and 4 women, age range 25–42 years) who were not subjected to any kind of treatment for the keloids. Six normal skin specimens were donated from each individual (1 man and 5 women, age range 28–45 years) who were under abdominal plastic resection and with no previous personal or family history of keloid scarring. All the samples were exclusively derived from abdominal keloids. Informed consent was obtained from each individual and the study was approved by the Ethics Committee of the Shanghai Jiao Tong University School of Medicine. All patient details are listed in Table 1.

Fibroblast isolation and culture from keloid and normal dermal tissue were established as previously described [20]. The primary to third passage cells were used in the following experiments.

Flow cytometry

FITC anti-human CD26 (BioLegend, USA) assay reagents were used to perform flow cytometry in this assay. The cell suspension was prepared at a density of 106 cells per 100 µL for each assay. 10 µL of anti-human CD26 reagent was added to each 100 µL cell suspension and then the sample was mixed. Afterwards the cells were incubated for 30 minutes at room temperature in the dark. Following incubation, stained cells were analysed by flow cytometry using 488 nm excitation and the green fluorescence emission was measured. The cell population could be separated into 2 groups: the $CD26^+$ cell population and the $CD26^-$ cell population. Six keloid samples and 6 normal skin samples were used and all the assays were performed in quadruplicate.

Generation of CD26 and IGF-1R-silenced KFs

To generate stably silenced KFs for CD26 and IGF-1R, lentiviral particles encoding shRNA targeting CD26 and IGF-1R (Hanbio Biotechnology Co., Ltd) were used for transfection. Briefly, when KFs were cultured to 50% confluence, the new culture medium containing puromycin (6 µg/ml) (Thermo Fisher Scientific, USA) was changed to the original medium, followed by the addition of a solution containing lentiviral particles for 24 hours at 37°C. Then cells were cultured in the medium containing puromycin (2 µg/ml) for 2 weeks to be selected for successful transformants. In addition, a scrambled control shRNA (Hanbio Biotechnology Co., Ltd, China), consisting of the same nucleotides in the shRNA but in random order and not matched to any other gene, was used as a control. RT-qPCR was employed to test the silencing efficiency of CD26 and IGF-1R in KFs.

Cell counting kit-8 cell proliferation assay

Cells were harvested at logarithmic phase, seeded in 96-well plates at a density of 1000 cells per well, along with 100 µL of medium, and incubated in a humidified incubator (37°C, 5% CO_2); the medium was changed every 48 hours. The culture medium was harvested and tested with a cell counting kit-8 (CCK-8; Dojindo, Japan) at 0, 24, 48, 72 and 96 hours. At each test time, 10 µL of sterile CCK-8 solution was added to each well and incubated for 2.5 hours at 37°C; the medium was then harvested for measuring the optical density values at 450 nm using a microplate reader (Thermo Electron Corporation, Finland). All the assays were performed in quadruplicate and repeated using 3 cell samples.

5-ethynyl-2′-deoxyuridine (EdU) incorporation assay

Cells were harvested at logarithmic phase, seeded in 96-well plates at a density of 4000 cells per well along with 5-ethynyl-20-deoxyuridine (BeyoClick™ EdU Cell Proliferation Kit Beyotime, China with Alexa Fluor 488) at a working concentration of 50 µM in 100 µL culture medium for 1 hour. The cells were washed twice in phosphate-buffered saline (PBS) for 5 minutes on each occasion, then fixed with 4%

Downloaded from academic.oup.com/burnstrauma/article/doi/10.1093/burnst/tkaa025/5943291 by guest on 15 October 2026

formaldehyde for 30 minutes at room temperature, permeabilized by incubation with 0.5 % Triton X-100 (Sigma; USA, 100 μL per well) in PBS for 10 minutes, following by staining with Hoechst (Beyotime; 1:100 dilution) for 10 minutes at room temperature. After the staining, the cells were imaged under a fluorescent microscope (Olympus, Japan). All the assays were performed in quadruplicate and repeated using 3 cell samples.

Cell migration assay

The cells were seeded uniformly (2×10^5 cells/well) into six-well plates and cultured for 24 hours. Plates were maintained at 37°C and 5% CO_2 in a moist atmosphere overnight to obtain a confluent cell monolayer. Cell wound scratches were made with a sterile 200 μL pipette tip and non-adherent cells were washed off with PBS, followed by culturation and incubation with non-supplemented fresh medium for 24 hours. The cell migration was observed at 0 and 24 hours and each well was photographed using objective inverted microscopy (Olympus, Japan). The photographed area was quantified by computer-assisted image analysis using IPP 6.0 (Media Cybernetics, USA) software. The results are presented as a percentage of the area of the scratch filled with the cells. The data were acquired from 4 randomly selected high-power fields.

All the assays were performed in quadruplicate and repeated using 3 cell samples.

Cell invasion assay

Transwell chambers coated with Matrigel (BD Biosciences, USA) were used to assess fibroblast invasion. Some 2×10^4 cells in 200 μL of serum-free DMEM medium were seeded on the upper chambers, and the lower chamber was filled with Dulbecco's modified Eagle's medium (DMEM, Gibco, USA) plus 10% FBS in a total volume of 500 μL. After 24 hours of culturation, the invaded cells that crossed the Matrigel barrier on the bottom surface of the membrane were fixed with methanol and stained with crystal violet. Images were taken using an inverted microscope. Invaded cells were photographed and counted by optical density of crystal violet stained cells. All the assays were performed in quadruplicate and repeated using 3 cell samples.

RT-qPCR

Total RNA was extracted from the cultured cells using TRIzol reagent (Invitrogen, USA), followed by treatment with DNase I (Promega Corp., USA). cDNA was synthesized with 2 μg total RNA in 30 μL of reaction buffer using a high-capacity cDNA synthesis kit (Takara Bio, Inc., Japan) according to the manufacturer's instructions. Gene expression data were detected using the ABI StepOnePlus system (Applied Biosystems®, Life Technologies). The thermal cycling parameters were 95°C for 1 minute, followed by 40 cycles of 95°C for 10 seconds and 60°C for 40 seconds. RT-qPCR was performed to detect mRNA levels using SYBR-Green I (Takara Bio, Inc.). The expression levels of genes were normalized to β-actin housekeeping gene expression. The primers used for RT-qPCR analysis were as follows: β-actin forward, 5′-GGCACTCTTCCAGCCTTCC-3′; β-actin reverse, 5′- GAGCCGCCGATCCACAC-3′; CD26 forward, 5′-GGGTCACATGGTCACCAGTG-3′; CD26 reverse, 5′- TCTGTGTCGTTAAATTGGGCATA-3′; IGF-1 forward, 5′-TCGACATCCGCAACGACTATC-3′; IGF-1 reverse, 5′- CCAGGGCGTAGTTGTAGAAGAG -3′. All RT-qPCR reactions were performed in triplicate. All the assays were performed in quadruplicate and repeated using 3 cell samples.

Western blot analysis

Cells were seeded into six-well plates with 2×10^5 cells/mL and cultured until confluence. After removal of the media, cells were washed twice with ice-cold PBS, then lysed using RIPA Lysis Buffer (Beyotime; 100 μL per test) and 1 mM phenylmethanesulfonyl fluoride (Beyotime) for 15 minutes. The lysates were collected by scraping from the plates, then centrifuged at 14,000 *g* at 4°C for 5 minutes. The extracted protein concentrations were quantified by Pierce™ BCA Protein Assay Kit (Thermo Scientific, USA) with the absorbance measured at a wavelength of 600 nm. The prepared protein was subjected to SDSPAGE and subsequently transferred onto PVDF membranes. The PVDF membrane was blocked with 5% non-fat powdered milk in Tris-buffered solution plus Tween-20 (TBST) for 2 hours at 37°C. Membranes were then incubated overnight at 4°C with primary antibodies. Rabbit polyclonal antibodies (anti-P-AKT, AKT, P-mTOR, mTOR, CD26; cell signalling; 1:1000), rabbit polyclonal antibodies to IGF1R, 70 kDa ribosomal protein S6 kinase (P70S6K), P-P70S6K, and P-4E-binding protein (4E-BP-1) (Cell Signaling Technology; USA,1:500) and mouse anti-β-actin (Sigma; USA, 1:5000) were used as primary antibodies. After washing 3 times in TBST for 10 minutes each time, membranes were incubated for 2 hours at room temperature with goat anti-rabbit/mouse secondary antibodies (cell signalling, 1:2000), followed by enhanced chemiluminescence (ECL) using a Pierce™ ECL Western Blotting Substrate (Thermo Fisher) according to the manufacturer's instructions. Image detection was conducted using the ImageQuant LAS 4000 miniature imaging system (GE Healthcare Bio-Sciences, USA). The results were normalized to β-actin where appropriate. All the assays were performed in quadruplicate and repeated using 3 cell samples.

ELISA assay

The cells were incubated in fibroblast complete medium to 80% confluency and then then washed and serum-starved for 24 hours. The released IGF-1 activities were measured using an ELISA kit (ExCell Bio, China). The data were measured at 490 nm using an ELISA analytical instrument (Molecular

Downloaded from academic.oup.com/burnstrauma/article/doi/10.1093/burnst/tkaa025/5943291 by guest on 15 October 2026

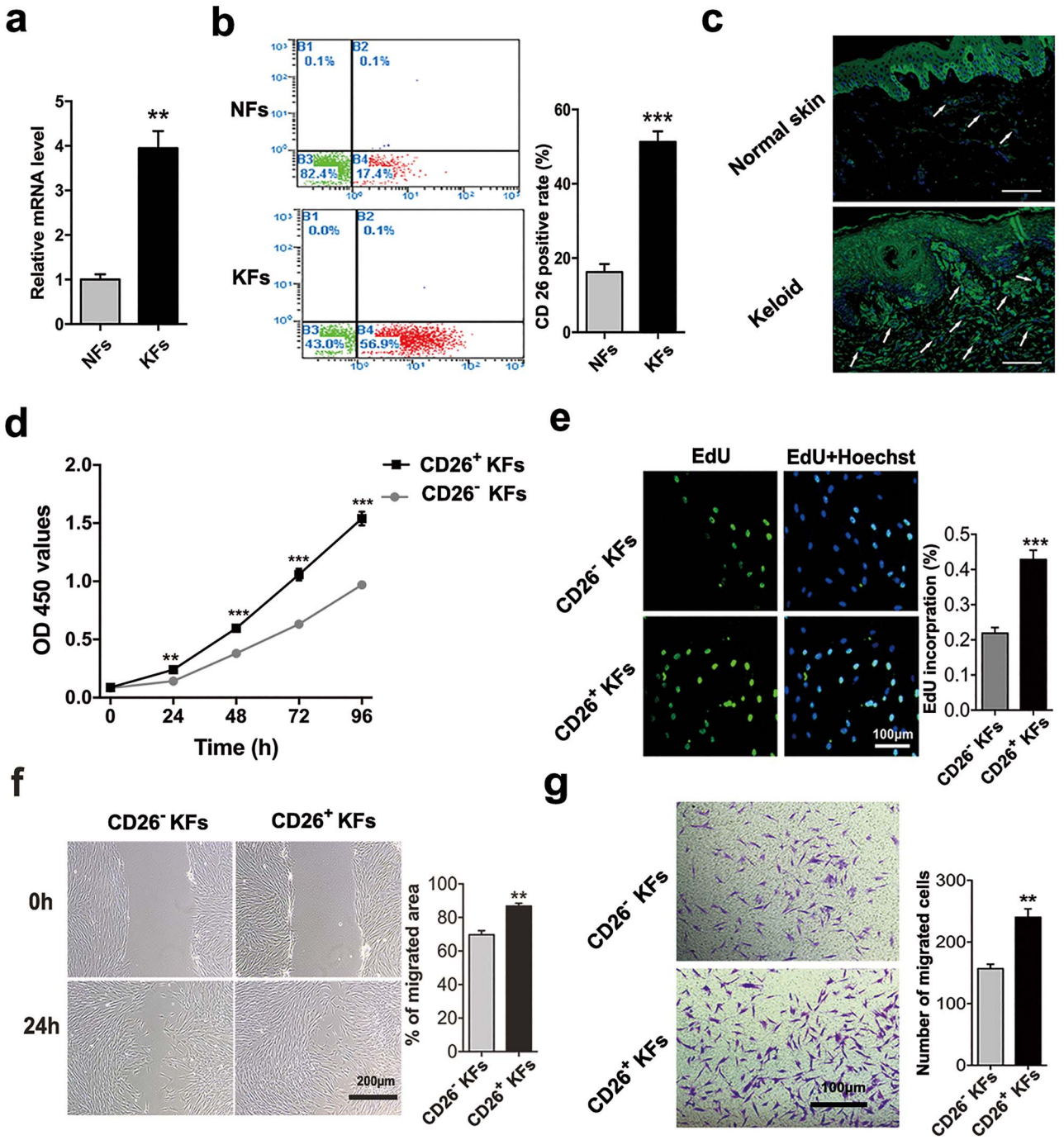

Figure 1. Cell proliferative and invasive abilities were upregulated in CD26^{+} keloid fibroblasts (KFs). **(a)** CD26 expressions in normal fibroblasts and KFs were analysed by RT-qPCR on mRNA level, the results showed that CD26 expression was upregulated in KFs. **(b)** CD26 expression on the cell surface was tested by flow cytometry. **(c)** Expressions of CD26 in human normal skin and keloid tissue were analysed by immunofluorescence staining. The white arrows point to CD26-positive staining. CD26 was obviously over-expressed in Keloid tissue compared to Normal skin tissue; bar = 100 μm. **(d)** Cell proliferation was measured with cell counting kit-8 assay at 0, 24, 48 and 96 hours, and CD26^{+} KFs showed an advantage in growth rate compared with CD26^{-} KFs. **(e)** EdU-positive rate was counted to evaluate cell growth activity, and CD26^{+} KFs showed higher positive rate than CD26^{-} KFs; bar = 100 μm. **(f)** CD26$^{+/-}$ KFs were grown to a confluent monolayer and scratched with a sterile pipette tip. The migrated area was counted with IPP software; bar = 200 μm. **(g)** CD26$^{+/-}$ KFs were seeded in the upper chamber (which had been coated with Matrigel), incubated for 24 hours and the invasive cells were visualized by staining with crystal violet; bar = 100 μm. Data are expressed as the mean ± standard error of the mean. $^{*}p < 0.05$, $^{**}p < 0.01$, $^{***}p < 0.001$. *NFs* normal fibroblasts

Devices; SpectraMax® Plus 384, USA). All the assays were performed in quadruplicate and repeated using 3 cell samples.

PI3K activity assay

PI3K activity was tested according to the PI3K activity detection kit (Echelon Biosciences, USA). PI3K was isolated and

Downloaded from academic.oup.com/burnstrauma/article/doi/10.1093/burnst/tkaa025/5943291 by guest on 15 October 2026

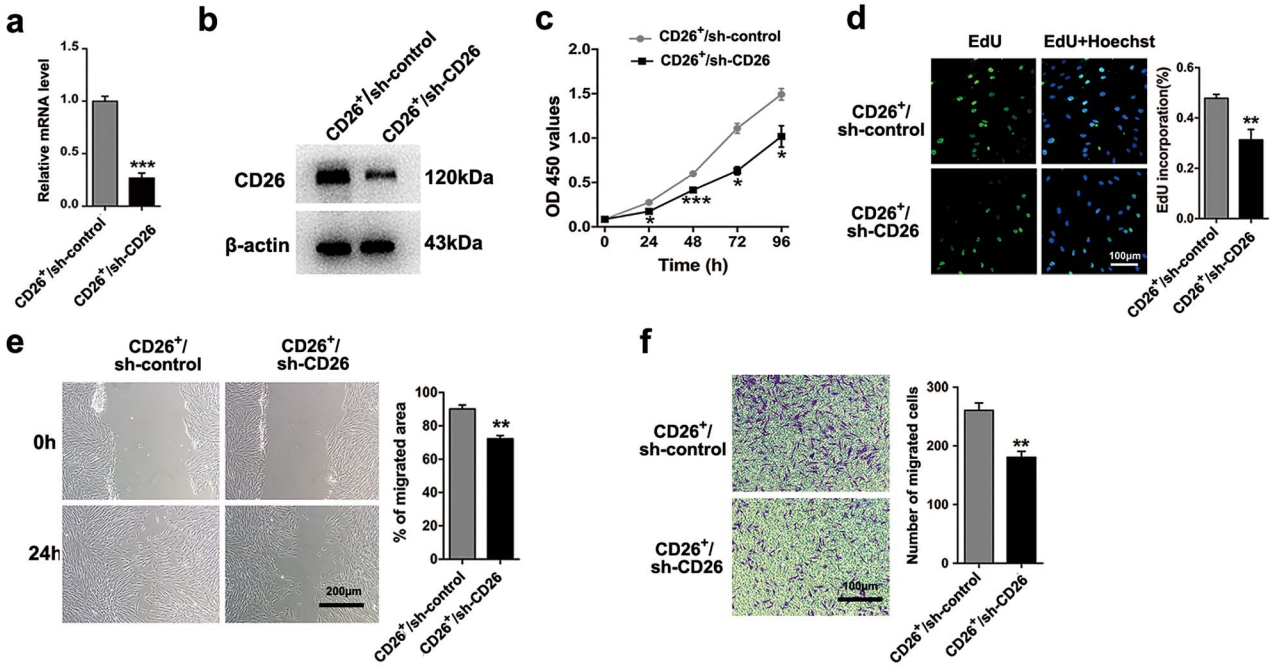

Figure 2. Effect of CD26 expression on the proliferative and invasive abilities of keloid fibroblasts (KFs). Verification of CD26 silencing in KFs using lentiviral-mediated transduction of shRNA specific for human CD26. **(a)** CD26 mRNA levels and **(b)** protein levels were determined using shRNA sequences specific for CD26 ($CD26^+$/sh-CD26) as well as a scrambled shRNA sequence ($CD26^+$/sh-control). **(c)** Cell counting kit-8 assay was used to test cell growth and the results showed that, after CD26 knock down, $CD26^+$/sh-CD26 showed a significantly slower growth rate than $CD26^+$/sh-control. **(d)** Cells stained with EdU were imaged under a fluorescent microscope; bar = 100 μm. **(e)** Cell migration was observed at 0 and 24 hours and the migration rates counted; bar = 200 μm. **(f)** A transwell assay was used to analyse cell invasion: observations showed that $CD26^+$/sh-control had a higher invasive ability than $CD26^+$/sh-CD26; bar = 100 μm. Data are expressed as the mean ± standard error of the mean. $^{**}p < 0.01$, $^{***}p < 0.001$. *$CD26^+$/sh-control* scrambled shRNA control group of $CD26^+$ keloid fibroblasts, *$CD26^+$/sh-CD26* keloid fibroblasts with CD26 knocked down

purified, then added to a substrate (1:1) for enzymatic reaction. The optical density (O.D.) were measured at 450 nm using an ELISA analytical instrument (Molecular Devices, SpectraMax® Plus 384), then the standard curve was plotted and the PI3K activity analysed according to the optical density (O.D.) values of the samples. All the assays were performed in quadruplicate and repeated using 3 cell samples.

Immunofluorescence staining

The cells were seeded in 12-well plates at a density of 4×10^4 cells per well. When the cells reached 70% confluence, they were fixed with 4% formaldehyde for 15 minutes at room temperature. Cells were blocked for 1 hour by 5% BSA (Gibco, USA) with 0.3% Triton X-100, then incubated with p-AKT primary antibody at 4°C overnight, following by treatment with Alexa Fluor488- or Alexa Fluor633-conjugated secondary antibodies (1:1000; Invitrogen) for 1 hour at 37°C. Images were captured using a laser confocal microscope (Leica TCS SP8; Leica, Germany). The images were obtained by scanning along the *Z* axis and the superposition was maximized using LAS AF Lite software to form two-dimensional images.

For tissue immunohistological staining, paraffin-embedded tissue sections were incubated with rabbit anti-CD26 (ab28340, Abcam), followed by incubation with a goat anti rabbit secondary antibody (111-545-003, Jackson ImmunoResearch, USA).

Statistical analysis

All data are presented as the mean ± standard error of the mean, and the statistical analyses were undertaken using GraphPad Prism6 software (La Jolla, USA). A Student's *t*-test (Gaussian distribution) was applied to compare the difference between the control and experimental groups. Statistical differences were considered significant at the $p < 0.05$ level.

Results

Aberrant expression of CD26 in KFs is associated with increased cell proliferative and invasive abilities

RT-qPCR and flow cytometric analysis were used to assess CD26 expression in NFs and KFs: the results revealed that CD26 expression was upregulated in KFs (Figures 1a, b). In addition, the expression of CD26 in keloid tissue was significantly higher than that in normal skin tissue, which is consistent with the flow cytometry results (Figures 1c). To analyse the proliferative ability of $CD26^{+/-}$ KFs, CCK-8 and EdU incorporation assays were performed: the results indicated that $CD26^+$ KFs showed an accelerated proliferation compared with $CD26^-$ KFs (Figures 1d, e). Meanwhile,

Downloaded from academic.oup.com/burnstrauma/article/doi/10.1093/burnst/tkaa025/5943291 by guest on 15 October 2026

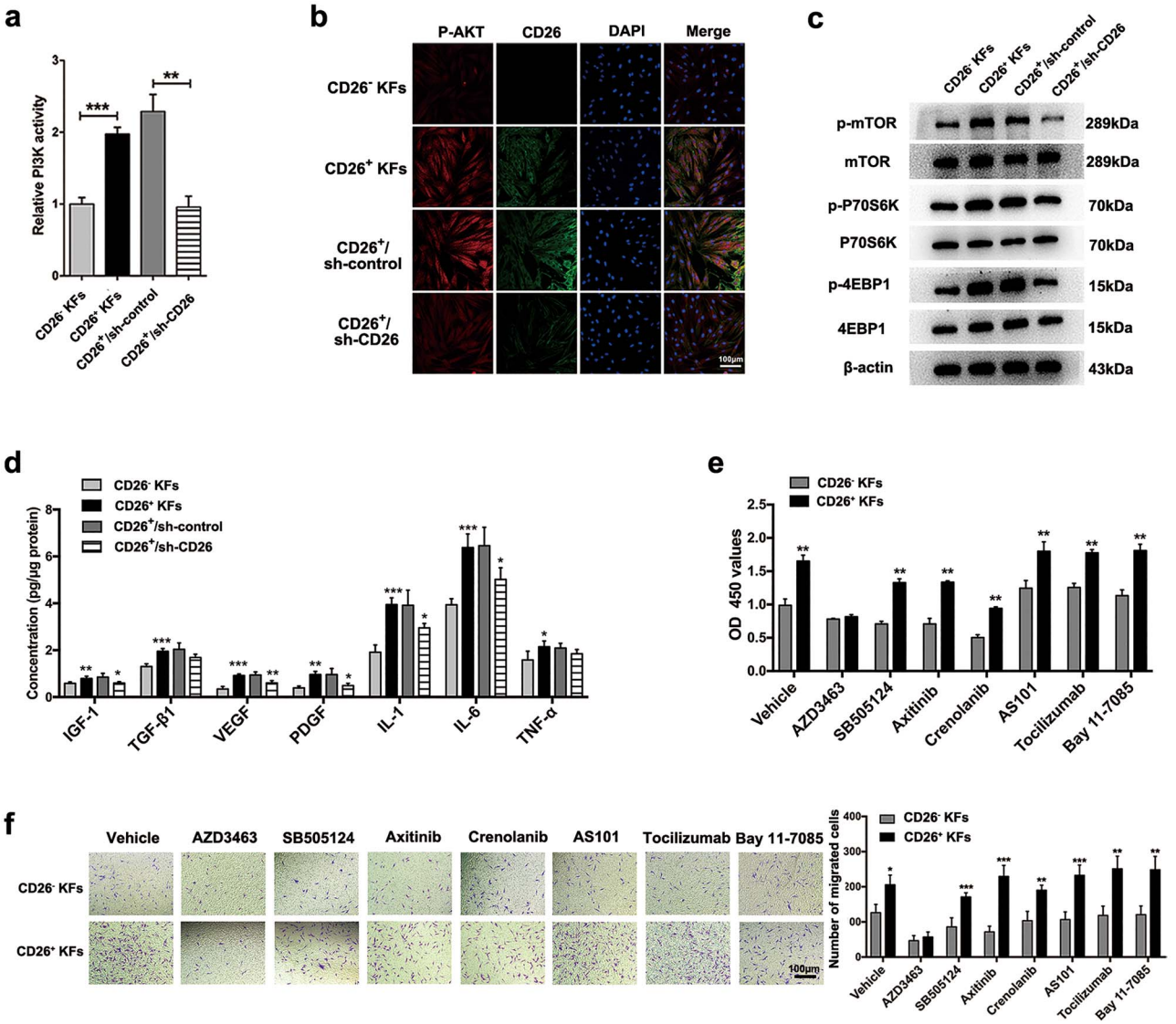

Figure 3. Effects of CD26 on signalling pathway of keloid fibroblasts (KFs) and screening of the related pathways. **(a)** The relationship between phosphatidylinositol 3-kinase (PI3K) activity and CD26 expression was in CD26$^+$ KFs and CD 26$^-$ KFs tested using a PI3K activity detection kit. **(b)** Protein kinase B (AKT) phosphorylation levels in CD26$^+$ KFs and CD26$^-$ KFs were detected and the samples were imaged under a fluorescent microscope; bar = 100 μm. **(c)** Cells were subjected to western blotting to determine the effects of CD26 expression on mammalian target of rapamycin and downstream molecular phosphorylation. **(d)** The expression of keloid-related cytokines in CD26$^{-/+}$ KFs was detected by ELISA assay. **(e)** CD26$^{-/+}$ KFs were cultured for 24 hours in the presence of insulin-like growth factor-1 receptor inhibitor AZD3463, transforming growth factor-β1 receptor inhibitor SB505124, vascular endothelial growth factor receptor inhibitor Axitinib, platelet-derived growth factor receptor inhibitor Crenolanib (CP-868596), interleukin-1β (IL-1β) inhibitor AS101, interleukin-6 receptor antagonist Tocilizumab and tumor necrosis factor-α inhibitor Bay 11-7085, respectively. The culture medium was then changed every 24 hours. Cell proliferation differences were analysed by cell counting kit-8 assay at 96 hours after seeding. **(f)** The invasive abilities of CD26$^{-/+}$ KFs were detected by transwell assay; bar = 100 μm. Data are expressed as the mean ± standard error of the mean. $^*p < 0.05$, $^{**}p < 0.01$, $^{***}p < 0.001$. *mTOR* mammalian target of rapamycin, *DAPI* 4′,6-diamidino-2-phenylindole, *OD* optical density

CD26$^+$ KFs displayed stronger migratory and invasive abilities compared with CD26$^-$ KFs (Figures 1f, g).

Then we knocked down CD26 in KFs using a lentiviral vector transfection system. To verify successful silencing of CD26 in KFs, we examined both the CD26 mRNA and protein expression levels in KFs with CD26 knocked down (CD26$^+$/sh-CD26) as well as a scrambled shRNA control group (CD26$^+$/sh-control) using RT-qPCR and western blot assay. The results showed that stable CD26-silenced KFs were generated (Figures 2a, b). The CD26$^+$/sh-CD26 had significantly reduced cell proliferative ability compared with the CD26$^+$/sh-control (Figures 2c, d). In addition, migration assay results showed that CD26$^+$/sh-CD26 had lower migration ability compared with the CD26$^+$/sh-control (Figure 2e). Similar results were observed in the invasion assay (Figure 2f). Taken together, our results demonstrated that CD26 expression in KFs could increase cell proliferative and invasive abilities.

Downloaded from academic.oup.com/burnstrauma/article/doi/10.1093/burnst/tkaa025/5943291 by guest on 15 October 2026

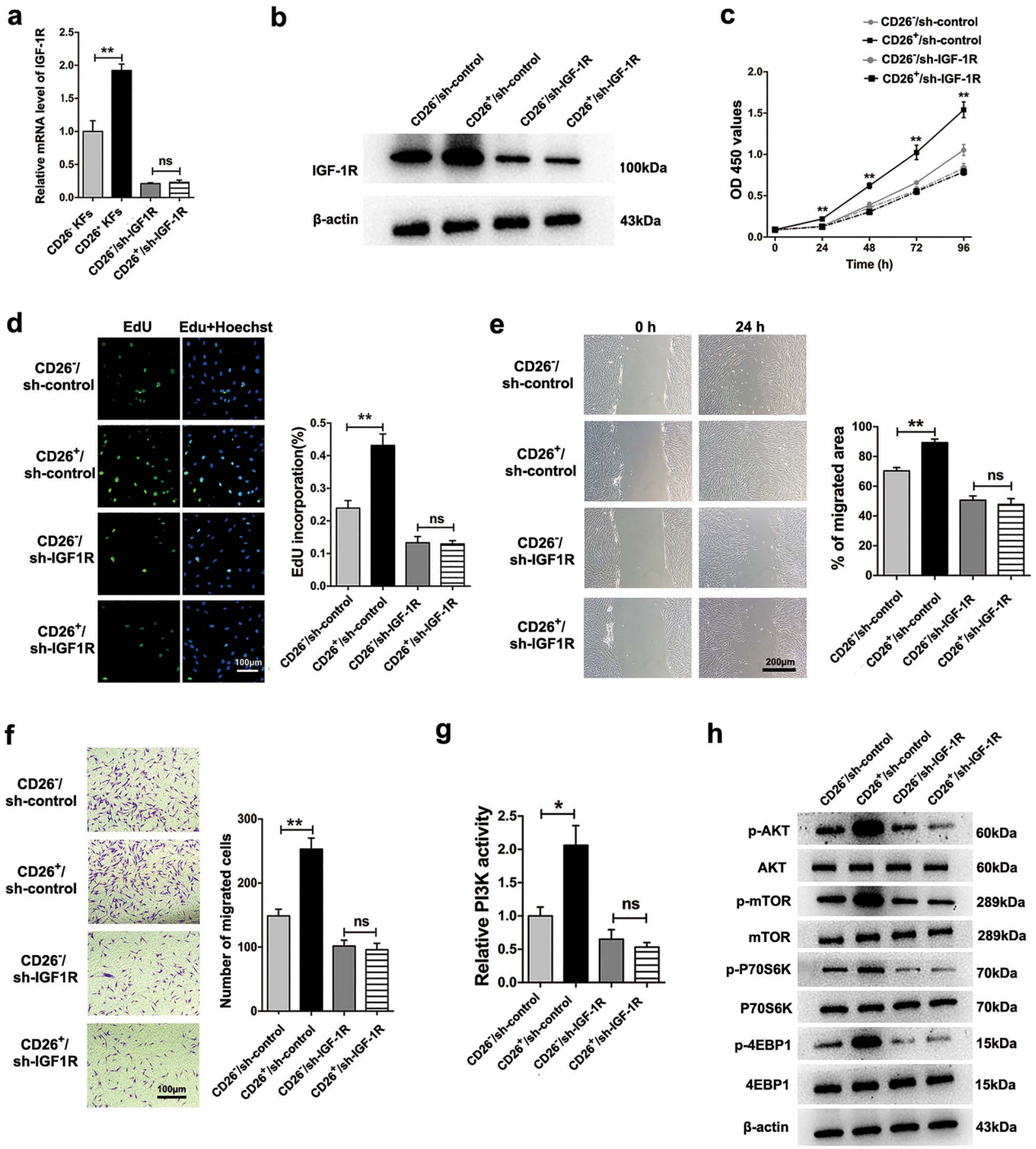

Figure 4. CD26 regulates the proliferation and invasion-related proteins of keloid fibroblasts (KFs) by insulin-like growth factor-1 receptor (IGF-1R). Verification of IGF-1R silencing in CD26$^{+/-}$ KFs using lentiviral-mediated transduction of shRNA specific for IGF-1R by RT-qPCR **(a)** and western blotting **(b)**. **(c)** Cell proliferative abilities were measured with cell counting kit-8 assay in CD26$^{+/-}$ KFs and IGF-1R-silenced CD26$^{+/-}$ KFs—the difference between CD26^{+} KFs and CD26^{-} KFs disappeared after IGF-1R was knocked down. **(d)** The EdU-positive rate was counted to evaluate cell growth activity: the difference between CD26^{+} KFs and CD26^{-} KFs was not observed after IGF-1R was knocked down. **(e)** The changes in CD26$^{+/-}$ KF migration after IGF-1R were knocked down were observed 24 hours after scratching and the percentage of the migrated area was measured. **(f)** The effects of IGF-1R knock down on CD26$^{+/-}$ KFs invasive abilities were observed. After IGF-1R was knocked down, **(g)** the phosphatidylinositol 3-kinase (PI3K) activities in CD26$^{+/-}$ KFs were detected. **(h)** The phosphorylation levels of PI3K were determined by western blotting. Data are expressed as the mean ± standard error of the mean. $^{*}p < 0.05$, $^{**}p < 0.01$. *CD26⁻/sh-IGF1R* stably silenced IGF-1Rs in CD26^{-} KFs, *CD26⁺/sh-IGF1R* stably silenced IGF-1Rs in CD26^{+} KFs, *CD26⁺/sh-control*, scrambled shRNA control group of CD26^{+} KFs, *P13K* phosphatidylinositol 3-kinase, *OD* optical density, *ns* no statistical difference

Downloaded from academic.oup.com/burnstrauma/article/doi/10.1093/burnst/tkaa025/5943291 by guest on 15 October 2026

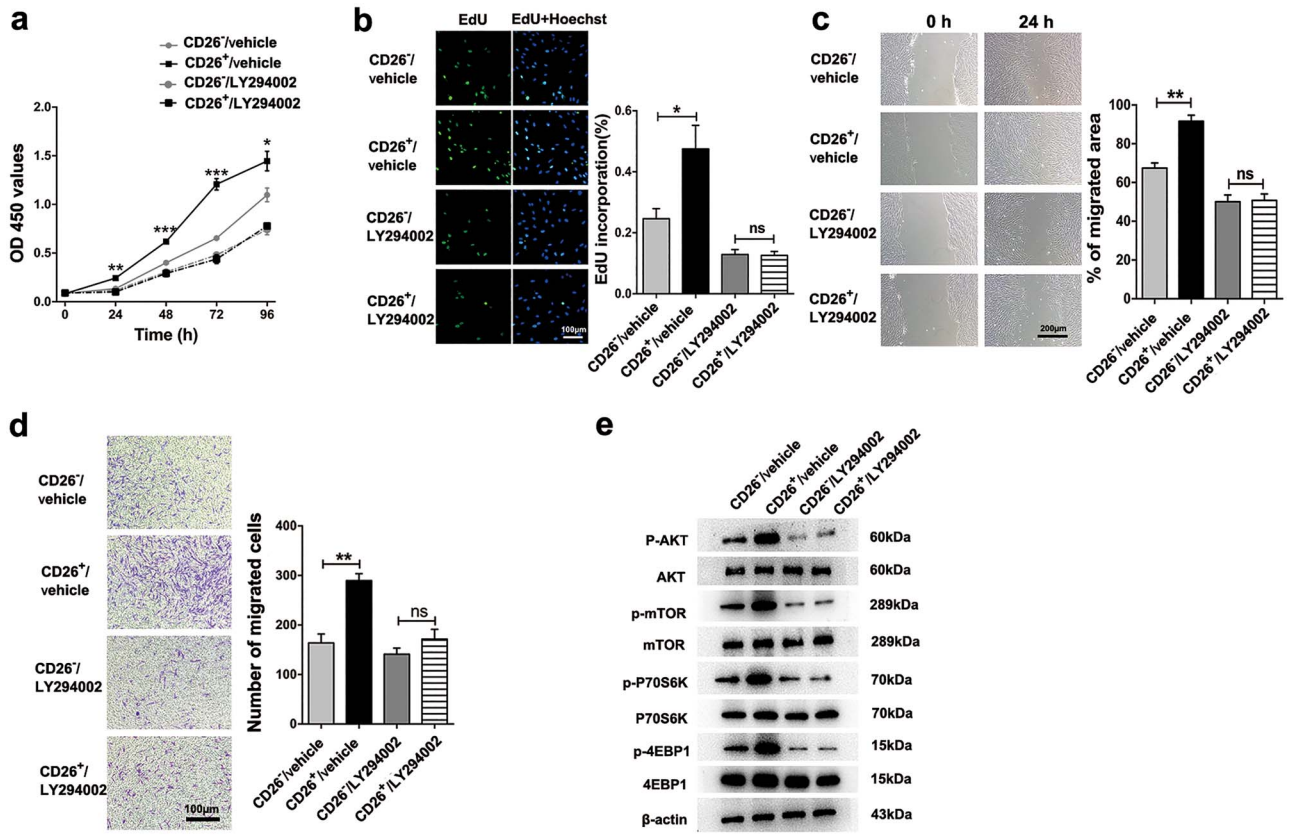

Figure 5. CD26 regulates the proliferative and invasive behaviours of keloid fibroblasts (KFs) by phosphatidylinositol 3-kinase (PI3K)/protein kinase B (AKT) activation in the insulin growth factor-1 (IGF-1)/IGF-1 receptor-mediated signalling pathway. The cell proliferation of $CD26^{+/-}$ KFs with or without PI3K inhibitor LY294002 (10 μM) treated for 24 hours, were then measured with cell counting kit-8 assay **(a)**, as well as EdU staining, the ratio of EdU-positive cells to Hoechst-labelled cells in each group was determined **(b)**. **(c)** The effect of PI3K on cell migration of $CD26^{+/-}$ KFs was evaluated after treatment with LY294002 (10 μM) for 24 h. **(d)** The changes in the invasive abilities of $CD26^{+/-}$ KFs after LY294002 treatment for 24 hours was observed. **(e)** The expression of molecules in the AKT pathway was tested by western blotting after treatment with LY294002. P70S6K: 70kDa ribosomal proteinS6 kinase. Data are expressed as the mean ± standard error of the mean. $^{*}p < 0.05$, $^{**}p < 0.01$, $^{***}p < 0.001$. *AKT* protein kinase B, *mTOR* mammalian target of rapamycin. *OD* optical density, *ns* no statistical difference

CD26 is associated with IGF-1/PI3K/AKT/mTOR pathway in keloids

PI3K activity in $CD26^{+}$ KFs was significantly increased compared to $CD26^{-}$ KFs, but after CD26 knocked down, PI3K activity was similar in both groups (Figure 3a). Compared to $CD26^{-}$ KFs, $CD26^{+}$ KFs increased phosphorylated AKT, indicating that CD26 could affect AKT phosphorylation and activation (Figure 3b). Similar results were observed in mTOR/P70S6K/4E-BP1 phosphorylation levels (Figure 3c). These results confirmed that the expression of CD26 affected the activation of the PI3K/AKT/mTOR pathway in KFs.

In the following experiments the key cytokines involved in the regulation of CD26 were analysed. First, the effect of the expression of the CD26 on the secretion level of keloid-related factors was analysed by knockout CD26 in KFs. The results showed that secretion levels of the detected cytokines were down-regulated after CD26 was knocked down in $CD26^{+}$ KFs, while the TGF-β1 and TNF-α secretion levels did not show significant difference (Figure 3d). Subsequently, $CD26^{+}$ KFs and $CD26^{-}$ KFs were treated with corresponding inhibitors of the cytokines to detect changes in cellular proliferation and invasion. The results showed that only after IGF-1R inhibitor was used did the differences in proliferation and invasion between $CD26^{+}$ KFs and $CD26^{-}$ KFs disappear, proving that the regulation of proliferation and invasion in KFs was achieved through the IGF-1/IGF-1R axis.

The role of IGF-1R in CD26-regulated KF proliferation and invasion-related signalling pathway

IGF-1 binding to IGF-1R leads to IGF-1R phosphorylation and insulin receptor substrate phosphorylation [26], which can activate PI3K and its downstream molecules AKT and mTOR. mTOR phosphorylates and activates S6 kinase 1 to phosphorylate downstream molecule ribosomal protein S6 and promotes protein translation. In addition, mTOR phosphorylates and inactivates eukaryotic initiation factor 4E-BP1, resulting in the release of inhibition on eIF4E, and promotes translation initiation.[30] To confirm the role of the IGF-1/IGF-1R axis in the CD26-regulating pathway, the IGF-1Rs in $CD26^{-}$ and $CD26^{+}$ KFs were

Downloaded from academic.oup.com/burnstrauma/article/doi/10.1093/burnst/tkaa025/5943291 by guest on 15 October 2026

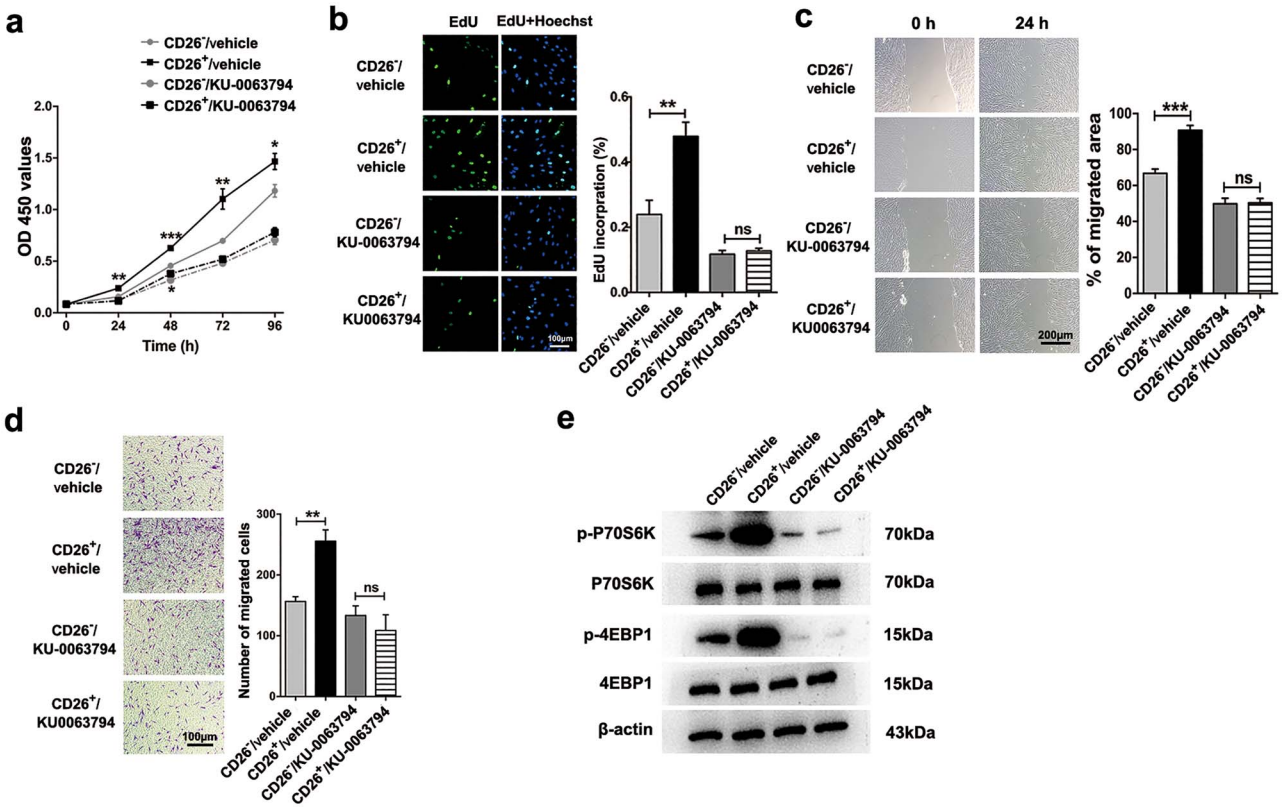

Figure 6. CD26 regulates the proliferative and invasive behaviours of keloid fibroblasts (KFs) by the mammalian target of rapamycin (mTOR) in the insulin-like growth factor-1 (IGF-1)–IGF-1 receptor (IGF-1R)/ phosphatidylinositol 3-kinase (PI3K)/protein kinase B (AKT)-mediated signalling pathway. The role of mTOR in the IGF-1–IGF-1R/PI3K/AKT activation of CD26$^+$ KFs was detected by treatment with mTOR inhibitor KU-0063794 (10 μM) for 24 h. **(a)** Cell counting kit-8 assay and **(b)** EdU staining showed that proliferation advantage in CD26$^+$ KFs did not remain after blockage of mTOR. **(c)** To evaluate the mTOR activation in cell migration regulation, a scratch wound was measured after 24 hours and there was no significant difference between the CD26$^+$ KFs treated with KU-0063794 (CD26$^+$/KU-0063794) and CD26$^-$ KFs treated with KU-0063794 (CD26$^-$/KU-0063794). **(d)** The invasive abilities of CD26$^{+/-}$ KFs were observed in transwell assay. **(e)** CD26 regulates the phosphorylation levels of S6 kinase and 4E-binding protein through IGF1R/PI3K/AKT/mTOR. Data are expressed as the mean ± the standard error of the mean. $^*p < 0.05$, $^{**}p < 0.01$, $^{***}p < 0.001$. *S6K* S6 kinase, *4EBP1* 4E-binding protein, *OD* optical density, *ns* no statistical difference

knocked down; the results revealed that stably silenced IGF-1Rs in CD26$^-$ KFs (CD26$^-$/sh-IGF1R) and CD26$^+$ KFs (CD26$^+$/sh-IGF1R) were established (Figures 4a, b). CCK-8 and EdU assays were used to analyse cell proliferation. In the CCK-8 assay there was a significant difference between the CD26$^-$ KFs and CD26$^+$ KFs; however, there was no proliferation difference between CD26$^-$/sh-IGF1R and CD26$^+$/sh-IGF1R, indicating that CD26 ceased regulation after the knockdown of IGF-1R (Figure 4c). Similar results were observed in the EdU assay (Figure 4d), and thus the results proved that CD26 upregulated the proliferation of KFs through IGF-1R. In the migration assay, after 24 hours' culturation the percentage coverage of the scratch area in CD26$^+$ KFs was higher than that in CD26$^-$ KFs, while this difference was not observed in the CD26$^-$/sh-IGF1R and CD26$^+$/sh-IGF1R groups, indicating that CD26 could mediate cell migration through IGF-1R (Figure 4e). Similarly, we also demonstrated that CD26 could regulate KF invasion ability through IGF-1R (Figure 4f). The role of IGF-1R in the PI3K pathway was further investigated. The PI3K activity was influenced by IGF-1R in CD26$^+$ KFs (Figure 4g). Next, we verified that the expression of IGF-1R could affect the phosphorylation level of the AKT/mTOR signalling pathway molecules in CD26$^+$ KFs (Figure 4h). Taken together, these results confirm that CD26 upregulated the KFs proliferation and invasion-related proteins by IGF-1/IGF-1R.

The effects of PI3K/AKT on CD26-regulated cell proliferation and the invasion-related signalling pathway

LY294002 was used as the inhibitor of PI3K/AKT in this assay. In the CCK-8 assay, the proliferative difference between CD26$^-$ and CD26$^+$ KFs was not observed after treatment with LY294002, indicating that CD26 could no longer work on KF proliferation once inhibited. PI3K/AKT activation was inhibited (Figure 5a). EdU staining also confirmed this conclusion (Figure 5b).

To evaluate the role of PI3K/AKT in cell migration and invasion, we observed the CD26$^{+/-}$ KF performances in control groups and LY294002-treated groups in wound scratch and transwell tests. CD26$^+$ KFs showed higher migratory and invasive capacity than CD26$^-$ KFs as expected, while this superiority disappeared after using LY294002, proving that CD26 could regulate cell migration and

Downloaded from academic.oup.com/burnstrauma/article/doi/10.1093/burnst/tkaa025/5943291 by guest on 15 October 2026

invasion through PI3K/AKT (Figures 5c, d). Moreover, the upregulated phosphorylation level of AKT downstream molecules in CD26$^+$ KFs disappeared after inhibiting PI3K/AKT activity (Figure 5e). Taken together, these results confirmed that CD26 affected cell proliferative and invasive behaviours by PI3K/AKT activation in the IGF-1/IGF-1R-mediated signalling pathway.

The effects of mTOR on CD26-regulated cell proliferation and the invasion-related signalling pathway

We next evaluated the role of mTOR in the CD26-mediated IGF-1- IGF1R/PI3K/AKT pathway in KFs. In this part, KU-0063794 was used as the inhibitor of mTOR. The proliferative difference between CD26$^-$ and CD26$^+$ KFs was observed. By contrast, there was no significant difference between the KU-0063794-treated CD26$^{-/+}$ KFs groups (Figure 6a, b). Consistent with the results of cell proliferation assays, the migration and invasion abilities of CD26$^+$ KFs were shown to be upregulated by mTOR (Figures 6c, d). The striking correlation between the CD26 expression and increase of p-P70S6K and 4E-BP1 was effectively inhibited by KU-0063794 treatment. The increased phosphorylation levels of S6K and 4E-BP1in CD26$^+$ KFs were inhibited after KU-0063794 treatment, further proving that CD26 regulated the phosphorylation levels of S6K and 4E-BP1 by activation of mTOR (Figure 6e). These results demonstrated that CD26 could affect cell proliferative and invasive behaviours by mTOR activation in the IGF-1–IGF-1R/PI3K/AKT-mediated signalling pathway.

In summary, the results demonstrated that CD26 activated the PI3K/AKT/mTOR pathway through IGF-1R to upregulate cell proliferation and invasion in keloids.

Discussion

KFs, the main inductive cells for keloid progression, are increasingly recognized as being heterogeneous. The site-specific characteristics in keloid tissue demonstrate the existence of subpopulations with different functions [31]; however, the lack of a valid biomarker leads to a failure to distinguish between the cell populations in keloid tissue.

First, we demonstrated that CD26 expression was increased in keloid patients. Then the role of CD26 in keloid progression was explored, and the results revealed that the CD26$^+$ KFs possess predominant proliferative and invasive characteristics promoting keloid progression [20]. Therefore, further exploration of the molecular mechanism underpinning this process was necessary.

We first knocked down CD26 in KFs to verify its role in the regulation of proliferation and migration (Figure 1). In comparison with CD26$^-$ KFs, CD26$^+$ KFs secreted more keloid-related cytokines, including IGF-1, TGF-β1, VEGF, PDGF, IL-1, IL-6 and TNF-α. CD26 expression influenced the secretion of these cytokines in KFs, but was not the key factor for TGF-β1 and TNF-α secretion in KFs (Figure 3d).

Then, in order to find out the key cytokine of CD26 regulation in KFs, the aforementioned cytokine inhibitors were applied to the experiments. The results showed that after treatment with the inhibitors of IL-1, IL-6 and TNFα, there was no significant decrease in the proliferation of CD26$^+$ KFs and CD26$^-$ KFs, and proliferative difference still existed between the two groups (Figure 3e). These data proved that IL-1β, IL-6 and TNFα have little effect on the cell proliferation of CD26$^+$ KFs and CD26$^-$ KFs. After treatment with the inhibitors of IGF-1, TGF-1, VEGF and PDGF, the proliferation of CD26$^+$ KFs and CD26$^-$ KFs decreased, indicating that these four cytokines are related to the upregulation of the proliferation apacity of CD26$^+$ KFs and CD26$^-$ KFs. However, only after in intervention of IGF-1R inhibitor AZD3463, the cellular proliferative difference between CD26$^+$ KFs and CD26$^-$ KFs disappeared, indicating that IGF-1 played a key role in the upregulation of CD26$^+$ KFs proliferation, and is the only core factor in the process of CD26-regulated KFs proliferation (Figure 3e). In the invasion experiment, the results showed that the cell invasion advantage of CD26$^+$ KFs disappeared only after the inhibition of IGF-1R, indicating that IGF-1 plays a key role in the process of CD26-regulated KF invasion (Figure 3f). These data indicate that the regulating effect of CD26 on proliferation and invasion in KFs was achieved through the IGF-1/IGF-1R axis. At present, many studies believe that TGF-β1 is the key cytokine regulating the pathological progress of keloid. Though the mechanism remains unclear, the upregulated expression of TGF-β1 may be closely related to the excessive collagen synthesis in keloid [13, 21, 22]. However, in our study, IGF-1-induced noncanonical TGF-β signalling was crucial to CD26$^+$ KF activation. Overexpression of IGF-1R in keloid meditates resistance to apoptosis leading to persistent proliferation and production of ECM [25]. Besides, IGF-1/IGF-1R was proved to mediate the invasiveness of KFs through the PI3K pathway [27, 32]. To demonstrate the role of the IGF-1/IGF-1R axis in the CD26 regulation process, we constructed IGF-1R-silenced CD26$^{+/-}$ KFs. The results showed that the proliferative and invasive advantage in CD26$^+$ KFs disappeared after IGF-1R was knocked down, confirming that CD26 mediated the cell activities through the IGF-1/IGF-1R axis (Figure 4).

The PI3K/AKT/mTOR pathway has been reported to be closely related to the pathophysiology of many types of human malignancies [33–35]. Hyperactivation of this pathway can be a result of mutations in the PI3K or AKT genes, loss of phosphatase and tensin homolog or constitutive activation of upstream regulatory pathways such as receptor tyrosine kinases [34, 35]. Previous studies have confirmed that mTOR was closely related to supernormal increased cell proliferation [36] and exceptional activation of AKT correlates with aggressive disease [37]. Using PI3K/AKT and mTOR inhibitors (Figures 5, 6), we verified the hypothesis

Downloaded from academic.oup.com/burnstrauma/article/doi/10.1093/burnst/tkaa025/5943291 by guest on 15 October 2026

that CD26 can activate the IGF-1/IGFR/PI3K/AKT/mTOR pathway leading to the upregulation of phosphorylated 4EBP1 and P70S6K, finally regulating cell growth and invasion in keloids.

In the present study, we focused on the modulatory action of CD26 on cell proliferation and invasiveness but did not study changes in collagen deposition. It has been reported that the abnormal balance between proliferation and apoptosis of KFs affects the deposition of ECM and invasion thereof into normal skin [38]. Therefore, in future work we will explore the relationship between CD26 expression and collagen deposition.

Previously, we identified CD26 as an effective marker for isolation of the main functional fibroblasts in keloid fibrogenesis. In the present study we confirmed that CD26 was closely related to cell proliferation and invasion regulation in KFs by establishing a stable CD26-silenced cell line (Figure 2). In our previous work, inhibition of CD26 was verified as effectively reducing fibrosis in keloids: it has been reported that CD26 inhibitors have potent immunosuppressive and anti-inflammatory effects in many pathological conditions [39], and some, such as sitagliptin and vildagliptin, have been approved by the FDA for the treatment of type 2 diabetes [40].

The IGF-1–IGF-1R/PI3K/AKT/mTOR pathway has become a target of interest for drug development given its role in many malignant tumours, and many agents used in clinical practice are designed to inhibit this pathway at different levels [41, 42]. Inhibition of PI3K pathway molecules has shown to exert a therapeutic effect against keloids, and more high-efficiency inhibitors need to be developed. Furthermore, development of such drugs, conducted in combination with the identification of a biomarker, will permit the selection of patients with a higher chance of response. Therefore, as an effective biomarker of KFs, CD26 may further promote the development of clinical treatment of keloids.

Conclusions

In the present study, CD26 was used to characterize a subpopulation of activated fibroblasts with increased proliferative and invasive abilities in keloids. CD26 was proven to upregulate KF proliferation and invasion through the IGF-1-induced PI3K/AKT/mTOR signalling pathway. Inhibition of both CD26 and the PI3K pathway exerts potent antifibrotic effects in keloid progression. These results may have direct implications as CD26 is a potential therapeutic target in keloid clinical treatment.

Abbreviations

ECM: extracellular matrix; KFs: keloid fibroblasts; NFs: normal fibroblasts; TGF- β1: transforming growth factor-β1; VEGF: vascular endothelial growth factor; PDGF: platelet-derived growth factor; IL-1: interleukin-1; IL-6: interleukin-6; TNF-α: tumor necrosis factor-α; IGF-1: insulin-like growth factor-1; IGF-1R: insulin-like growth factor-1 receptor; PI3K: phosphatidylinositol 3-kinase; AKT: protein kinase B; mTOR: mammalian target of rapamycin; CCK-8: cell counting kit-8; PBS: phosphate-buffered saline; TBST: Tris-buffered solution plus Tween-20; ECL: enhanced chemiluminescence; CD26$^+$/sh-CD26: KFs with CD26 knocked down; CD26$^+$/sh-Control: scrambled shRNA control group of CD26$^+$ KFs; CD26$^-$/sh-IGF1R: stably silenced IGF-1Rs in CD26$^-$ KFs; CD26$^+$/sh-IGF1R: stably silenced IGF-1Rs in CD26$^+$ KFs

Funding

This study was supported by the National Natural Science Foundation of China (81772098, 81801917, 81801918), the Outstanding Professional and Technical Leader Program of the Shanghai Municipal Science and Technology Commission (18XD1423700), the Clinical Multi-Disciplinary Team Research Program of 9th People's Hospital, Shanghai Jiao Tong University School of Medicine (2017-1-007), the Clinical Research Program of 9th People's Hospital, Shanghai Jiao Tong University School of Medicine (JYLJ027), the Shanghai Municipal Education Commission Gaofeng Clinical Medicine Grant Support (20152227) and the project of Science and Technology Commission of Shanghai Municipality (17411952800, 18441904500).

Availability of data and materials

The datasets used and/or analysed in the current study are available from the corresponding author upon reasonable request.

Authors' contributions

XY performed the study, analysed the data and drafted the manuscript. PRM and HX analysed the data. Corresponding authors YXZ, YZ and ZZ contributed to the conceptual design of the study, interpreted the data, provided funding support and critically revised the manuscript. All authors have given final approval and agree to be accountable for all aspects of the work.

Ethics approval and consent to participate

This study was approved by the Ethics Committee of Shanghai Jiao Tong University School of Medicine.

Conflicts of interest

The authors declare that they have no conflicts of interest.

References

1. Niessen FB, Spauwen PH, Schalkwijk J, Kon M. On the nature of hypertrophic scars and keloids: a review. *Plast Reconstr Surg*. 1999; 104: 1435–58.

Downloaded from academic.oup.com/burnstrauma/article/doi/10.1093/burnst/tkaa025/5943291 by guest on 15 October 2026

2. Vincent AS, Phan TT, Mukhopadhyay A, Lim HY, Halliwell B, Wong KP. Human skin keloid fibroblasts display bioenergetics of cancer cells. *J Invest Dermatol*. 2008; 128: 702–9.
3. Wang W, Qu M, Xu L, Wu X, Gao Z, Gu T, *et al*. Sorafenib exerts an anti-keloid activity by antagonizing TGF-beta/Smad and MAPK/ERK signaling pathways. *J Mol Med (Berl)* 2016; 94: 1181–94.
4. Shih B, Garside E, McGrouther DA, Bayat A. Molecular dissection of abnormal wound healing processes resulting in keloid disease. *Wound Repair Regen*. 2010; 18: 139–53.
5. Zhang Z, Nie F, Kang C, Chen B, Qin Z, Ma J, *et al*. Increased periostin expression affects the proliferation, collagen synthesis, migration and invasion of keloid fibroblasts under hypoxic conditions. *Int J Mol Med*. 2014; 34: 253–61.
6. Srivastava S, Kumari H, Singh A. Comparison of fractional CO2 laser, verapamil, and triamcinolone for the treatment of keloid. *Adv Wound Care (New Rochelle)*. 2019; 8: 7–13.
7. Feng JJ, See JL, Choke A, Ooi A, Chong SJ. Biobrane™ for burns of the pubic region: minimizing dressing changes. *Military Med Res*. 2018;5:29.
8. Lee YS, Hsu T, Chiu WC, Sarkozy H, Kulber DA, Choi A, *et al*. Keloid-derived, plasma/fibrin-based skin equivalents generate de novo dermal and epidermal pathology of keloid fibrosis in a mouse model. *Wound Repair Regen*. 2016; 24: 302–16.
9. Ghazizadeh M, Tosa M, Shimizu H, Hyakusoku H, Kawanami O. Functional implications of the IL-6 signaling pathway in keloid pathogenesis. *J Invest Dermatol*. 2007; 127: 98–105.
10. Yu C, Xu ZX, Hao YH, Gao YB, Yao BW, Zhang J, et al. A novel microcurrent dressing for wound healing in a rat skin defect model. *Mil Med Res*. 2019; 6(1):22.
11. Ashcroft KJ, Syed F, Bayat A. Site-specific keloid fibroblasts alter the behaviour of normal skin and normal scar fibroblasts through paracrine signalling. Site-specific keloid fibroblasts alter the behaviour of normal skin and normal scar fibroblasts through paracrine signalling.PLoS One. 2013;8(12):e75600. doi: 10.1371/journal.pone.0075600
12. Rinkevich Y, Walmsley GG, Hu MS, Maan ZN, Newman AM, Drukker M, *et al*. Identification and isolation of a dermal lineage with intrinsic fibrogenic potential. *Science*. 2015; 348: aaa2151.
13. Mah W, Jiang G, Olver D, Gallant-Behm C, Wiebe C, Hart DA, *et al*. Elevated CD26 expression by skin fibroblasts distinguishes a Profibrotic phenotype involved in scar formation compared to gingival fibroblasts. *Am J Pathol*. 2017; 187: 1717–35.
14. Leavitt T, Hu MS, Marshall CD, Barnes LA, Lorenz HP, Longaker LMT. Scarless wound healing: finding the right cells and signals. *Cell Tissue Res*. 2016; 365: 483–93.
15. Mulvihill EE, Drucker DJ. Pharmacology, physiology, and mechanisms of action of Dipeptidyl Peptidase-4 inhibitors. *Endocr Rev*. 2014; 35: 992–1019.
16. Ohnuma K, Nam HD, Chikao M. Revisiting an old acquaintance: CD26 and its molecular mechanisms in T cell function. *Trends Immunol*. 2008; 29: 295–301.
17. Krakauer. M, Sorensen PS , Sellebjerg F. CD4(+) memory T cells with high CD26 surface expression are enriched for Th1 markers and correlate with clinical severity of multiple sclerosis. *J Neuroimmunol*. 2006; 181: 157–64.
18. K E, Y U, C S, T O, H N, K M, *et al*. Increment in the Ta1+ cells in the peripheral blood and thyroid tissue of patients with Graves' disease. *J Immunol*. 1989; 142.
19. Alina S, Hermina AG, Alexandru EM, Clara D, Simon R, Thomas W, *et al*. Dipeptidyl-peptidase-4 as a marker of activated fibroblasts and a potential target for the treatment of fibrosis in Systemic Sclerosis. Hoboken, N.J.: Arthritis & rheumatology, 2020; 72: 137–149.
20. Alina S, Hermina AG, Alexandru EM, Clara D, Simon R, Thomas W, et al. Dipeptidyl-peptidase-4 as amarker of activated fibroblasts and a potential target for the treatment of fibrosis in Systemic Sclerosis. Hoboken, N.J.: Arthritis & rheumatology, 2020;72:137–149.
21. Györfi AH, Matei A-E, Distler JHW. Targeting TGF-β signaling for the treatment of fibrosis. *Matrix Biol*. 2018; 8: 68–9.
22. Hong S-K, Choo E-H, Ihm S-H, Chang K, Seung K-B. Dipeptidyl peptidase 4 inhibitor attenuates obesity-induced myocardial fibrosis by inhibiting transforming growth factor-βl and Smad 2/3 pathways in high-fat diet-induced obesity rat model. *Metabolism*. 2017; 76: 42–55.
23. Chen J, Alberts I, Li X. Dysregulation of the IGF-I/PI3K/AKT/mTOR signaling pathway in autism spectrum disorders. *Int J Dev Neurosci*. 2014; 35: 35–41.
24. Shih B, Bayat A. Genetics of keloid scarring. Genetics of keloid scarring. *Arch Dermatol Res*. 2010; 302: 319–39.
25. Ishihara H, Yoshimoto H, Fujioka M, Murakami R, Hirano A, Fujii T, *et al*. Keloid fibroblasts resist ceramide-induced apoptosis by overexpression of insulin-like growth factor I receptor. *J Invest Dermatol*. 2000; 115: 1065–71.
26. Laviola L, Natalicchio A, Giorgino F. The IGF-I signaling pathway. *Curr Pharm Des*. 2007; 13: 663–9.
27. Yoshimoto H, Ishihara H, Ohtsuru A, Akino K, Murakami R, Kuroda H, *et al*. Overexpression of insulin-like growth factor-1 (IGF-I) receptor and the invasiveness of cultured keloid fibroblasts. *Am J Pathol*. 1999; 154: 883–9.
28. Xue G, Hemmings BA. PKB/Akt-dependent regulation of cell motility. PKB/Akt-dependent regulation of cell motility. *J Natl Cancer Inst*. 2013; 105: 393–404.
29. Syed F, Sherris D, Paus R, Varmeh S, Singh S, Pandolfi PP, *et al*. Keloid disease can be inhibited by antagonizing excessive mTOR signaling with a novel dual TORC1/2 inhibitor. *Am J Pathol*. 2012; 181: 1642–58.
30. Beugnet A, Wang X, Proud CG. Target of rapamycin (TOR)-signaling and RAIP motifs play distinct roles in the mammalian TOR-dependent phosphorylation of initiation factor 4E-binding protein 1. *J Biol Chem*. 2003; 278: 40717–22.
31. Lu F, Gao J, Ogawa R, Hyakusoku H, Ou C. Biological differences between fibroblasts derived from peripheral and central areas of keloid tissues. *Plast Reconstr Surg*. 2007; 120: 625–30.
32. Song J, Xu H, Lu Q, Xu Z, Bian D, Xia Y, *et al*. Madecassoside suppresses migration of fibroblasts from keloids: involvement of p38 kinase and PI3K signaling pathways. *Burns*. 2012; 38: 677–84.
33. Thorpe LM, Yuzugullu H, Zhao JJ. PI3K in cancer: divergent roles of isoforms, modes of activation and therapeutic targeting. *Nat Rev Cancer*. 2015; 15: 7–24.
34. Engelman JA. Targeting PI3K signalling in cancer: opportunities, challenges and limitations. *Nat Rev Cancer*. 2009; 9: 550–62.
35. Courtney KD, Corcoran RB, Engelman JA. The PI3K pathway as drug target in human cancer. *J Clin Oncol*. 2010; 28: 1075–83.
36. Steelman LS, Chappell WH, Abrams SL, Kempf RC, Long J, Laidler P, *et al*. Roles of the Raf/MEK/ERK and PI3K/PTEN/Akt/mTOR pathways in controlling growth and sensitivity to therapy-implications for cancer and aging. *Aging (Albany NY)*. 2011; 3: 192–222.

Downloaded from academic.oup.com/burnstrauma/article/doi/10.1093/burnst/tkaa025/5943291 by guest on 15 October 2026

37. Wegiel B, Bjartell A, Culig Z, Persson JL. Interleukin-6 activates PI3K/Akt pathway and regulates cyclin A1 to promote prostate cancer cell survival. *Int J Cancer.* 2008; 122: 1521–9.
38. Luo S, Benathan M, Raffoul W, Panizzon RG, Egloff DV. Abnormal balance between proliferation and apoptotic cell death in fibroblasts derived from keloid lesions. *Plast Reconstr Surg.* 2001; 107: 87–96.
39. Jung FJ, Yang L, De Meester I, Augustyns K, Cardell M, Hillinger S, *et al.* CD26/dipeptidylpeptidase IV-targeted therapy of acute lung rejection in rats. *J Heart Lung Transplant.* 2006; 25: 1109–16.
40. Ahren B. DPP-4 inhibitors. *Best Pract Res Clin Endocrinol Metab.* 2007; 21: 517–33.
41. Ocana A, Amir E, Seruga B, Martin M, Pandiella A. The evolving landscape of protein kinases in breast cancer: clinical implications. *Cancer Treat Rev.* 2013; 39: 68–76.
42. Garcia-Echeverria C, Sellers WR. Drug discovery approaches targeting the PI3K/Akt pathway in cancer. *Oncogene.* 2008; 27: 5511–26.

Downloaded from academic.oup.com/burnstrauma/article/doi/10.1093/burnst/tkaa025/5943291 by guest on 15 October 2026